— 16 —

White Light Inter-calibrations of UVCS, LASCO-C2 and Spartan 201/WLC

RICHARD A. FRAZIN
Harvard-Smithsonian Center for Astrophysics, Cambridge, MA, USA

MARCO ROMOLI
Dip. di Astronomia e Scienza dello Spazio
Università di Firenze, Firenze, Italy

JOHN L. KOHL, LARRY D. GARDNER
Harvard-Smithsonian Center for Astrophysics, Cambridge, MA, USA

DENNIS WANG, RUSSELL A. HOWARD
E.O. Hulburt Center for Space Research
Naval Research Laboratory, Washington, DC, USA

THERESE A. KUCERA
NASA Goddard Space Flight Center, Greenbelt, MD, USA

This paper describes comparisons among white light polarized radiances (pB) as measured by the Ultraviolet Coronagraph Spectrometer White Light Channel (UVCS/WLC), the Large Angle and Spectrometric Coronagraph Experiment C2 instrument (LASCO-C2) and the Spartan 201 White Light Coronagraph (Spartan 201/WLC). UVCS/WLC and LASCO-C2 are generally in agreement, although there are some systematic trends and discrepancies that still require explanation. UVCS/WLC and Spartan 201/WLC agree to within the measurement uncertainties. Spartan 201/WLC and LASCO-C2 are not directly compared to each other in this paper.

16.1 Introduction

The UVCS White Light Channel (UVCS/WLC; *Kohl et al.* [1995]), the Large Angle and Spectrometric Coronagraph Experiment C2 instrument (LASCO-C2; *Brueckner et al.* [1995]), and the Spartan 201 White Light Coronagraph (Spartan 201/WLC; *Fisher and Guhathakurta* [1994]) all measure the polarized radiance (pB) of the solar corona. In this paper we present a systematic comparison of their pB measurements. A paper that describes the calibration of Spartan 201/WLC and a direct inter-comparison of LASCO-C2 and the Spartan 201/WLC is in preparation [*Kucera*, 2002].

Although the UVCS/WLC calibration is still in progress, for the purposes of this paper we adopt the in-flight calibration that is described in *Romoli et al.* [2002], which also gives

a brief summary of the UVCS/WLC and its characteristics. The LASCO-C2 calibration has been described by *Howard et al.* [2002].

16.2 Observations

We present two types of comparisons of UVCS/WLC and LASCO-C2. The first type is based on special observations that were designed specifically for the purpose of intercalibration. The second type of comparison is based on synoptic observations, which are part of the daily observation program of both UVCS and LASCO. The UVCS synoptic program is described by *Panasyuk* [1999]. The UVCS/WLC to LASCO-C2 comparisons based on special observations were made at a larger range of heights, have better spatial co-registration (at least in the cases when the star ρ Leo was used as a pointing marker, see below), have smaller time differences between the UVCS/WLC and LASCO-C2 exposures, and allow more time for the UVCS mirror mechanism to settle (see below). However, the comparison based on synoptic observations is valuable because it has many more data points (about 17 000 UVCS/WLC pBs), which have been taken in the same systematic way throughout the mission. Unlike the special observations, the UVCS/WLC synoptic data set includes observations of coronal holes. We also present a comparison of UVCS/WLC and Spartan 201/WLC, which required special observations on the part of UVCS.

The special observations for the UVCS/WLC to LASCO-C2 comparisons were taken in August and September 1996, during the ρ-Leo solar crossings of August 1999 and 2000, and in early April 2000. The special observations for the UVCS/WLC to Spartan comparison were taken during the STS-95 John Glenn shuttle mission in early November 1998. The observations used for synoptic comparisons come from the years 1996 through 2000.

All of the LASCO-C2 data used for the comparisons presented here were multiplied by 0.8 in order to renormalize them to Sun-center radiance (as opposed to mean-Sun). This operation was not required for the Spartan 201 data because they were already normalized to the Sun-center value.

Any externally occulted coronagraph is subject to vignetting, that is, the effective aperture of the instrument is a function of position in the field of view. Since the UVCS/WLC instrument has a linear occulter and the optics are believed to be uniform, the vignetting function is proportional to the exposed mirror area ($h_m w_m(r)$ in *Romoli et al.* [2002]). LASCO-C2 and Spartan 201 have circular occulters and their vignetting functions are much more complicated.

The LASCO-C2 vignetting function is derived from laboratory measurements and from observing the irradiances of stars passing through the field of view. The vignetting function is 1.0 at the edge of the field (about 6 $R_\odot$), and approaches 0.0 near 2.3 $R_\odot$. From 2.5 to 4.0 $R_\odot$ the vignetting function goes from 0.1 to 0.45 [*Wang*, 2001].

All of the UVCS/WLC pB values were corrected for stray light, as described in *Romoli et al.* [2002]. The stray light correction is not necessarily just a matter of subtracting a background because the background may be *negative*. The coronal pB (in the appropriate coordinate system) is equal to the Q-component of the Stokes vector and is positive. The Q-component of the stray light signal may be positive or negative. The analysis of *Romoli et al.* [2002] shows that for the UVCS/WLC, the stray light contribution to Q is positive

and Table 4 in *Romoli et al.* [2002] gives the values that must be subtracted.

Since the UVCS/WLC selects different position angles in the corona by rotating about an axis, the occulting geometry and instrumental stray light are nearly independent of position angle. There is a slight variation of the occulting geometry due to the fact that the roll ring is not perfectly circular [*Frazin*, 2002]. This causes pointing changes on the order of $15''$, which have been taken into account in the UVCS Data Analysis Software (DAS). This pointing correction was included in the inter-comparison work presented here.

The roll offset described above changes the alignment between the occulting system and the Sun. Both the observations taken in the spring of 2000, in which the pointing stages were used to compensate for the roll offset, and the stray light analysis used in *Romoli et al.* [2002] show that these small variations do not affect the stray light correction.

All of the UVCS/WLC pB measurements, both special and synoptic, have been corrected for a mirror mechanism nonlinearity and an electronic mirror-grating cross-talk effect, both of which affect the pointing. The mirror-grating cross-talk effect has been discussed in detail by *Fineschi et al.* [1997]. The calibration of the mirror mechanism nonlinearity was done with UV observations of the star ρ Leo [*Frazin*, 2002]. This calibration accounted for the SOHO-Earth parallax, which is necessary because the SOHO-Earth vector affects the position of the star relative to the Sun. Such pointing considerations are important because the UVCS/WLC is a 1-pixel instrument with a projected image of $14''$ by $14''$. The UVCS pointing analysis shows that the position of the WLC pixel can be located within a standard uncertainty of $20''$.

The UVCS special observations taken during the ρ-Leo solar crossings of 1999 and 2000 did not rely on the pointing analysis because they used the star as a pointing marker (in fact, these observations are the basis of the UVCS pointing analysis). In these cases the pointing of the UVCS instrument was determined from the star's UV signature in the O VI channel, the alignment of which to the WLC is known. The UVCS/WLC was not pointed at the star; it made measurements of the corona. The UVCS/WLC radiometric measurements of ρ Leo described in *Romoli et al.* [2002] come from a separate set of observations.

The UVCS mirror mechanism has a temperature sensitivity that can affect the pointing. About an hour is required for the mechanism to reach equilibrium. This effect sometimes manifests after large changes in the roll angle, which can cause a rearrangement of the temperature gradients in the instrument. Care has been taken to ensure that this effect does not have any important consequences for pB measurement. Exposures taken at the three rotation angles of the half-wave retarder plate (HWRP) must measure the emission from the same spatial location of the corona. Since the UVCS special observations, except for those used in the Spartan 201 comparison, involved spending enough time at one roll angle for the mechanism to settle, the mechanism settling causes no problems. Most of the UVCS/WLC special observations used for the Spartan 201 comparison also allowed sufficient time to reach equilibrium. Those with short exposure times (60 s, 180 s per pB cycle) sometimes allowed less time for settling. All of the measurements taken with short exposures show very little evidence of problems associated with mechanism settling (which manifests as jitter in time series plots). Thus, we do not expect any effects due to settling in these data.

The original synoptic observation plan was designed before the mirror settling problem was discovered. The synoptic plan was changed in March 1999 to address this concern. The new synoptic plan has a shorter pB sequence (i.e., a set of exposures using three

HWRP orientations) and takes several sequences at each height. Comparisons of the pB values from the old and new synoptic plans show no differences for heights above 2.0 $R_\odot$. Furthermore, comparisons of the pBs from the old synoptic sequences to observations at the same height and roll angle with sufficient settling time show no clear differences, either. Analysis has shown that the settling time for the pB sequences in the original synoptic plan was short enough to eliminate the settling problem.

The comparisons presented here suffer, by varying degrees, from a lack of temporal co-registration between observations of the instruments involved. The corona varies on all temporal scales [e.g., *Solanki*, 2002] and it is difficult to characterize this variation. There is no doubt that some of the scatter in the comparison plots is due to a lack of simultaneity. The UVCS/WLC to LASCO-C2 comparisons based on synoptic observations are simultaneous to within 12 hours or less; the data with larger time differences were not used. The UVCS/WLC to LASCO-C2 comparisons of special observations have much better temporal co-registration due to efforts made to coordinate LASCO-C2 and UVCS. These efforts involved taking extra pB sequences on the part of LASCO-C2. For the 1996 comparison, the time differences are 5 hours or less. For the 1999 ρ-Leo passage, 3 of the data points (i.e., sets of joint pB observations at common spatial locations and times) have time differences of about 2, 2, and 3 hours. The other 8 have differences of about an hour or less. For the 2000 ρ-Leo comparison, two of the data points have time differences of about 11 and 7 hours. The other five have time differences of 3 hours or less. For the Spring 2000 comparison, efforts were made to take LASCO-C2 pB sequences both before and after the UVCS/WLC pB sequences, "sandwiching" the UVCS/WLC pBs within a 2 hour time span. This was successful for 7 of the 8 data points. In the other case, there is a LASCO-C2 observation about 3 hours before the UVCS/WLC pB and another about 24 hours later. For the UVCS/WLC to Spartan comparison, the time differences vary between 14 and 0 hours, with 6 (the squares in Figure 16.6) of the 19 data points having time differences of 2 hours or less.

16.3 Uncertainty Analyses

Below we present four types of measured quantities. These are UVCS/WLC pBs, LASCO-C2 pBs, ratios of (UVCS/WLC pB)/(LASCO-C2 pB), and ratios of (UVCS/WLC pB)/(Spartan 201 pB). In this section we quantify the uncertainties in each. All uncertainties are treated statistically as random sign errors and stated for approximately the standard uncertainty level (i.e., 68 % confidence).

16.3.1 UVCS/WLC pB Uncertainty

A major contributor to the uncertainty in UVCS/WLC pBs is the 7 % radiometric uncertainty in the in-flight calibration, described in *Romoli et al.* [2002]. The accuracy of the polarimetry has also been discussed there and we associate no significant uncertainty with this aspect of the measurement.

Correcting for stray light introduces uncertainty into the UVCS/WLC pB measurements. The fractional uncertainty is given by $\delta Q_s/(Q_m - Q_s)$, where Q_m is the measured pB before stray light correction, Q_s is the value of the stray light correction that needs to be subtracted, and δQ_s is the uncertainty in the stray light correction. The values of Q_s

and δQ_s as a function of radius are given in Table 4 in *Romoli et al.* [2002]. For both the UVCS/WLC to LASCO-C2 and the UVCS/WLC to Spartan comparisons based on special observations (i.e., those shown in Figures 16.1 and 16.6), this uncertainty was calculated individually for each data point and is reflected in the error bars. However, in order to give the reader an understanding of the size of these corrections, we take the time to discuss some averages.

Above 2 $R_\odot$, the mean of $\delta Q_s/Q_s$ from Table 4 in *Romoli et al.* [2002] is 0.57 and the standard deviation is 0.13. The median of $Q_s/(Q_m - Q_s)$ for the UVCS/WLC data used in Figure 16.1 (which contains 30 data points) is 0.13; the mean is 0.19, and the standard deviation is 0.15. By multiplying $< \delta Q_s/Q_s >$ ($< >$ indicates that the mean is to be taken) by the median of the $Q_s/(Q_m - Q_s)$ distribution, we get a measure of the size of the uncertainty in the UVCS/WLC correction. Thus, we have $0.57 \times 0.13 \approx 0.07$, and the median relative standard uncertainty is about 7 %. The uncertainty due to the UVCS/WLC stray light correction in observations used for the UVCS/WLC to Spartan comparison is highly variable. The maximum value of $0.57 \times Q_s/(Q_m - Q_s)$ (recalling that $< \delta Q_s/Q_s >= 0.57$, as discussed above) is 0.76 (the next highest are 0.35 and 0.21), the minimum is 0.01, the median is 0.04, the mean is 0.12, and the standard deviation is 0.19. Thus, we take the median relative standard uncertainty due to instrument stray light for the UVCS/WLC to Spartan pB comparison to be 4 %.

The uncertainty due to the stray light correction was similarly calculated for the synoptic observations. At position angles of 0° and 180° at 2.6 $R_\odot$ the average relative standard uncertainty due to the stray light correction is 6 % and the standard deviation is 1 %. At position angles of 90° and 270° at 2.7 $R_\odot$ the average relative standard uncertainty is 2 % and the standard deviation is 1 %, and at 3.0 $R_\odot$ the average is 5 % and the standard deviation is 2 %.

The uncertainty in the UVCS/WLC vignetting is determined by the standard uncertainty in the location of the internal occulter, which is 0.1 mm. At the lowest height used in this paper, about 1.6 $R_\odot$, the exposed mirror width is about 1.6 mm, giving a relative standard uncertainty of 6.25 %. At 2.1 $R_\odot$, the exposed mirror width is about 5.6 mm, giving a relative standard uncertainty of 1.8 %, and it is even smaller at larger heights. The 1.6 $R_\odot$ measurement is only used for the Spartan 201 comparison, and 6 % is negligible compared to the 20 % Spartan 201 radiometric relative standard uncertainty. We have shown that it is negligible compared to other uncertainties and we will not consider it further.

This analysis is summarized in Table 16.1.

16.3.2 LASCO-C2 pB Uncertainty

The LASCO-C2 radiometric calibration is based on measurements of stars that drift through the field of view. The residuals have a standard deviation of about 3 %, and we take this to be the radiometric relative standard uncertainty. The LASCO-C2 CCD flat-field has been determined by closing the door in front of the telescope and taking images of the door diffuser. The result is that the flat-field is uniform to within 2 % [*Wang*, 2001].

The amount of polarized stray light in LASCO-C2 is difficult to determine and work in this area is still in progress. However, since the C2 and C3 coronagraphs agree in their overlap region (above 4 $R_\odot$), in both coronal holes and streamers, and C3 has a much larger

source	resulting uncertainty in pB
radiometry	7 %
stray light (special obs., LASCO-C2 comparison (2.4 – 5.0 $R_\odot$), median)	7 %
stray light (special obs., Spartan comparison (1.7 – 4.3 $R_\odot$), median)	4 %
stray light (synoptic obs., 0° & 180°, 2.6$R_\odot$, mean)	6 %
stray light (synoptic obs., 90° & 270°, 2.7$R_\odot$, mean)	2 %
stray light (synoptic obs., 90° & 270°, 3.0$R_\odot$, mean)	5 %
quadrature sum (special obs., LASCO-C2 comparison (2.4 - 5.0 $R_\odot$), median)	10 %
quadrature sum (special obs., Spartan comparison (1.7 - 4.3 $R_\odot$), median)	8 %
quadrature sum (synoptic obs., 0° & 180°, 2.6$R_\odot$, mean)	9 %
quadrature sum (synoptic obs., 90° & 270°, 2.7$R_\odot$, mean)	7 %
quadrature sum (synoptic obs., 90° & 270°, 3.0$R_\odot$, mean)	9 %

Table 16.1: Summary of relative standard uncertainties in UVCS/WLC pB measurements. Angles refer to the position angle which is measured counter-clockwise from the projection of solar north.

occulting disk, it may be that C2 stray light is not a significant issue for the comparisons reported here.

The accuracy of the LASCO-C2 vignetting function has been tested by watching the star ρ Leo pass through the field of view. The corrected irradiance of the star is flat to about 8 % from 2.9 to 6 $R_\odot$. Inside of 2.9 $R_\odot$ the vignetting function needs improvement, with the star 30 % dimmer than expected at the edge of the occulter near 2.5 solar radii. Since the star track is just one line through the field of view the problem of correcting the entire field of view remains [*Wang*, 2001].

For lack of a better procedure, we assign an 8 % vignetting relative standard uncertainty to the LASCO-C2 pBs above 2.9 $R_\odot$, and 30 % below.

This analysis is summarized in Table 16.2.

source	resulting uncertainty in pB
radiometry	3 %
flat-field	2 %
vignetting (above 2.9 $R_\odot$)	8 %
vignetting (below 2.9 $R_\odot$)	30 %
quadrature sum (above 2.9 $R_\odot$)	9 %
quadrature sum (below 2.9 $R_\odot$)	30 %

Table 16.2: Summary of relative standard uncertainties in LASCO-C2 pB measurements.

16.3.3 UVCS/WLC to LASCO-C2 pB Ratio Uncertainty

The uncertainty in the UVCS/WLC to LASCO-C2 pB ratio is a combination of the uncertainties described in the previous two sections plus additional uncertainties due to inaccurate spatial and temporal co-registration. Since we have no way to estimate the uncertainty due to inaccurate temporal co-registration, we do not attempt to do so. There

is no doubt that some of the scatter in the UVCS/WLC to LASCO-C2 pB ratio plots is due to a lack of simultaneity, however this should not produce any systematic trends.

The uncertainty due to inexact spatial co-registration is more readily analyzed. The LASCO-C2 pixel position standard uncertainty is on the order of $10''$ and the standard uncertainty in the UVCS pointing analysis is about $20''$. In order to evaluate the importance of this pointing uncertainty we found the LASCO-C2 pB pixel that matched our best determination of the position of the UVCS/WLC and looked at the values in the surrounding $1'$ by $1'$ (3 pixel by 3 pixel) box of the LASCO-C2 pB image. We took the standard deviation of these 9 pB values divided by their mean value as the relative standard uncertainty due to co-registration. We repeated this procedure 10 times at heights ranging from 2.6 to 4.0 $R_\odot$. The mean of the 10 values is 0.055 and the standard deviation is 0.0285 due to co-registration; thus we take the relative standard uncertainty in the UVCS/WLC to LASCO-C2 pB ratio to be (5.5 ± 2.9) %.

This analysis is summarized in Table 16.3.

source	resulting uncertainty in pB
UVCS/WLC radiometry	7 %
UVCS/WLC stray light (special obs., LASCO-C2 comparison (2.4 – 5.0 $R_\odot$), median)	7 %
UVCS/WLC stray light (synoptic obs., 0° & 180°, 2.6$R_\odot$, mean)	6 %
UVCS/WLC stray light (synoptic obs., 90° & 270°, 2.7$R_\odot$, mean)	2 %
UVCS/WLC stray light (synoptic obs., 90° & 270°, 3.0$R_\odot$, mean)	5 %
LASCO-C2 radiometry	3 %
LASCO-C2 flat-field	2 %
LASCO-C2 vignetting (above 2.9 $R_\odot$)	8 %
LASCO-C2 vignetting (below 2.9 $R_\odot$)	30 %
spatial co-registration	5.5 %
quadrature sum (below 2.9 $R_\odot$)	32 %
quadrature sum (above 2.9 $R_\odot$, non-coronal hole)	15 %

Table 16.3: Summary of relative standard uncertainties in the UVCS/WLC to LASCO-C2 pB ratios. Angles refer to the position angle which is measured counter-clockwise from the projection of solar north. No uncertainty due to temporal co-registration has been included in the quadrature sums (see text).

16.3.4 UVCS/WLC to Spartan 201 pB Ratio Uncertainty

The Spartan 201 relative standard uncertainty in radiometry is reported to be 20 % [*Kucera*, 2002], and this dominates the uncertainty in the comparison to UVCS/WLC. The Spartan 201 stray light uncertainty is still in progress, but 10 % is probably an upper limit because the dynamic range of the Spartan 201 pB data used to produce Figure 16.6 is about 10 at 1.7 $R_\odot$. Since the Spartan 201 images can be co-registered with those of LASCO-C2 to a high degree of accuracy, we use the spatial co-registration relative standard uncertainty of 5.5 % given in the previous section. Since we have no way to estimate the uncertainty due to inaccurate temporal co-registration, we do not attempt to do so. There is no doubt that some of the scatter in Figure 16.6 is due to a lack of simultaneity, however this should not produce any systematic trends. This analysis is summarized in Table 16.4.

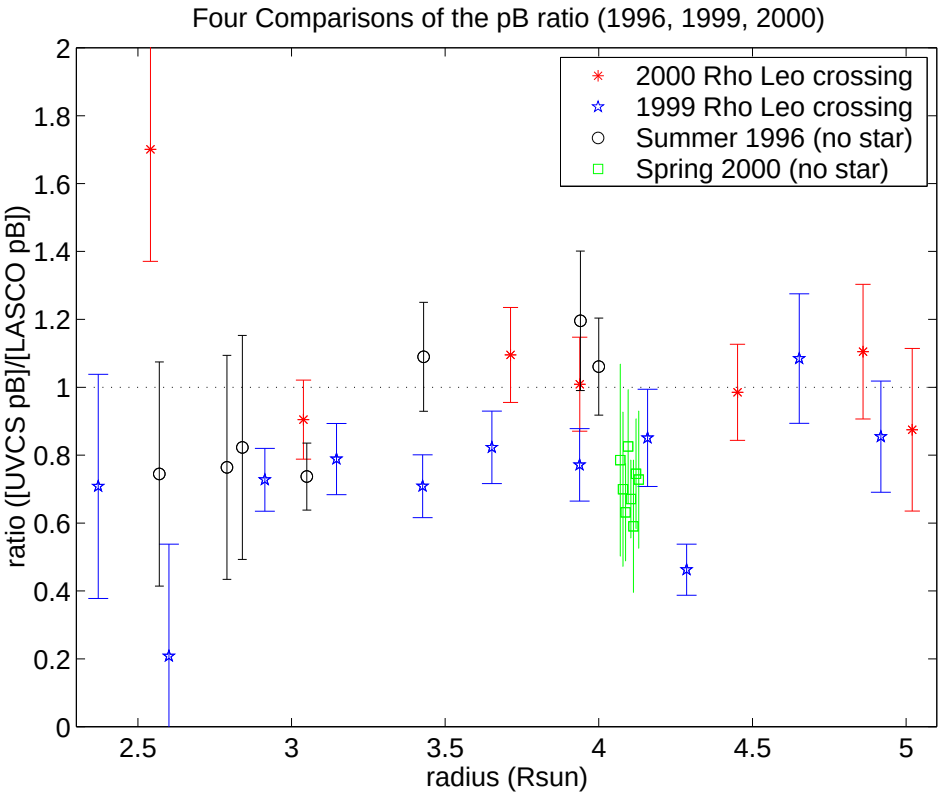

Figure 16.1: Four comparisons of the UVCS/WLC to LASCO-C2 pB ratio. See text for details.

16.4 Results

16.4.1 UVCS/WLC and LASCO-C2: Special Observations

Figure 16.1 shows the results of the UVCS/WLC and LASCO-C2 comparison based on special observations. It consists of four different data sets. The error bars represent the 17 % and 33 % relative standard uncertainties from Table 16.3. The four different data sets depicted in Figure 16.1 are as follows:

1. The black circles represent data taken on 20 August and 1 September 1996. The ratios range from about 0.65 to 1.2.

2. The blue pentagrams represent data taken at the time of the ρ-Leo crossing in August 1999. ρ Leo was used as a pointing marker to aid in co-registration. Except for three outliers, the ratio is between 0.65 and 0.85.

3. The red asterisks represent data taken during the ρ-Leo crossing in August and September 2000. Again, ρ Leo was used as a pointing marker. Except for one

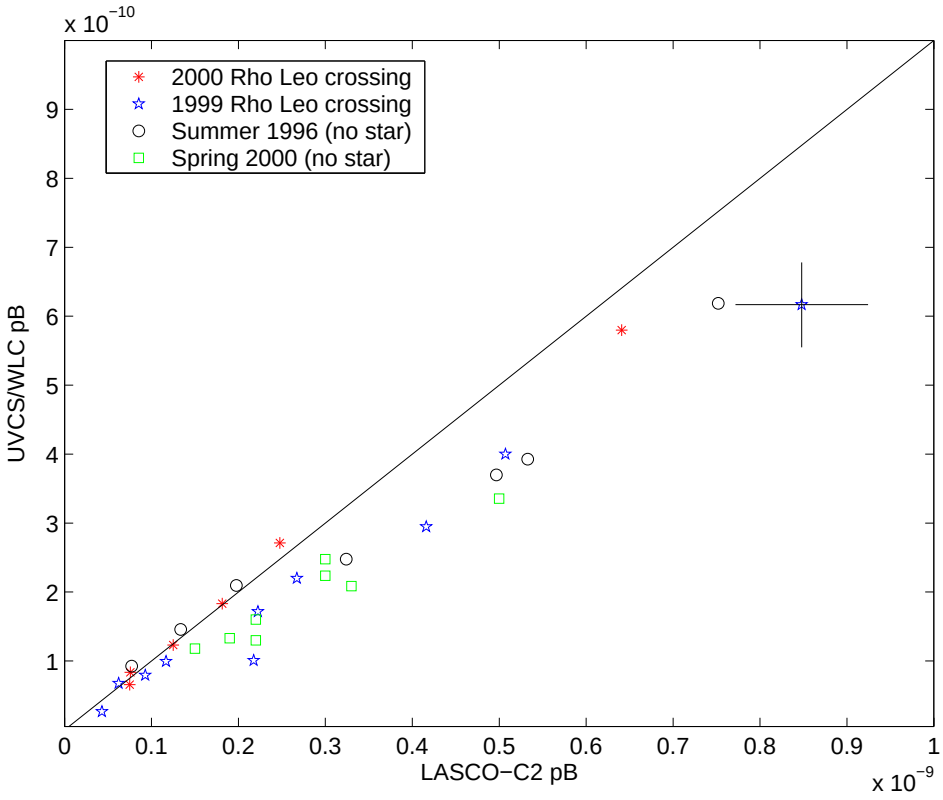

Figure 16.2: Scatter plot corresponding to the four comparisons in Figure 16.1. The error bars shown are representative of the sample. An uncertainty analysis is given in the text. Several outliers from Figure 16.1 are not shown here.

outlier, the ratios vary from about 0.85 to 1.1, and are all larger than the 1999 ρ-Leo ratios.

4. The green squares represent data taken in April 2000 at 4.15 $R_\odot$ (spread out for display). These ratios cluster around 0.7 and vary from about 0.55 to 0.8.

The median of all the ratios in Figure 16.1 is 0.79, the mean is 0.84 and the standard deviation is 0.25.

Figure 16.2 is a plot of LASCO-C2 pB versus UVCS/WLC pB corresponding to the data points in Figure 16.1, except that three of the 34 points are missing. These three points are the outliers in Figure 16.1 and have not been included in order to have a smaller scale of the display. Error bars are only given for one of the data points. The relative standard uncertainties in both the UVCS/WLC and LASCO-C2 measurements are representative of the sample. For more details on the uncertainties see Section 16.3.

source	resulting uncertainty in pB ratio
UVCS/WLC radiometry	7 %
UVCS/WLC stray light (median)	4 %
Spartan 201 radiometry	20 %
spatial co-registration	5.5 %
quadrature sum (median)	22 %

Table 16.4: Summary of relative standard uncertainties in the UVCS/WLC to Spartan 201 pB ratios. No uncertainty in temporal co-registration has been included in the quadrature sum (see text).

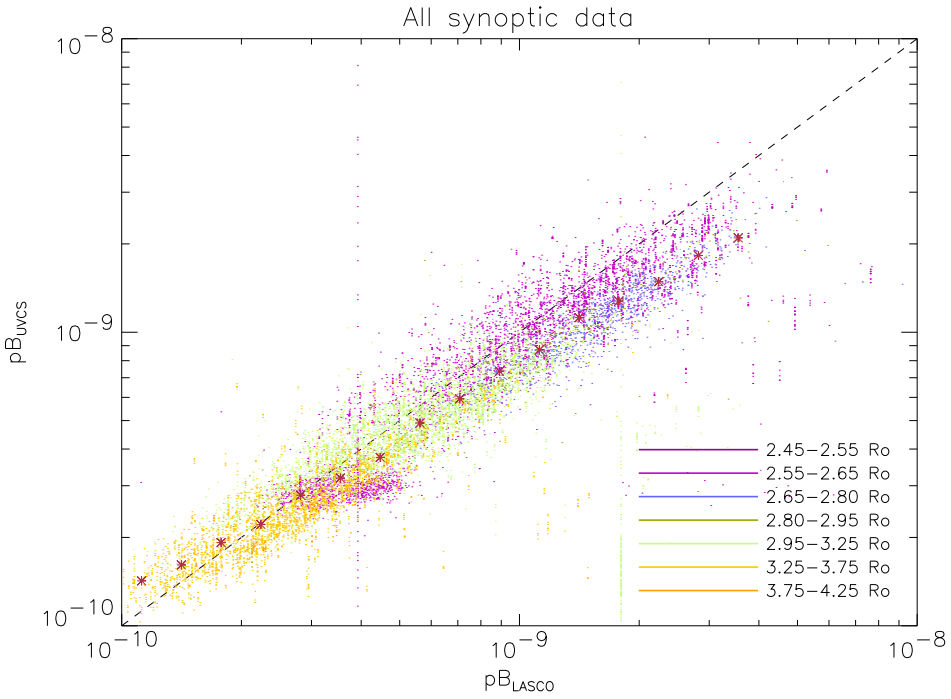

Figure 16.3: Scatter plot for all synoptic data. The LASCO-C2 pB is plotted on the x-axis and the UVCS/WLC pB is plotted on the y-axis. Different colors are used for data taken at different heights. The asterisks represent the median of the distribution.

16.4.2 UVCS/WLC and LASCO-C2: Synoptic Observations

Figure 16.3 is a plot of LASCO-C2 pB versus UVCS/WLC pB for the selected synoptic data. The asterisks represent the median of the distribution. As the figure shows, the median value of the UVCS/WLC to LASCO-C2 pB ratio decreases with signal strength.

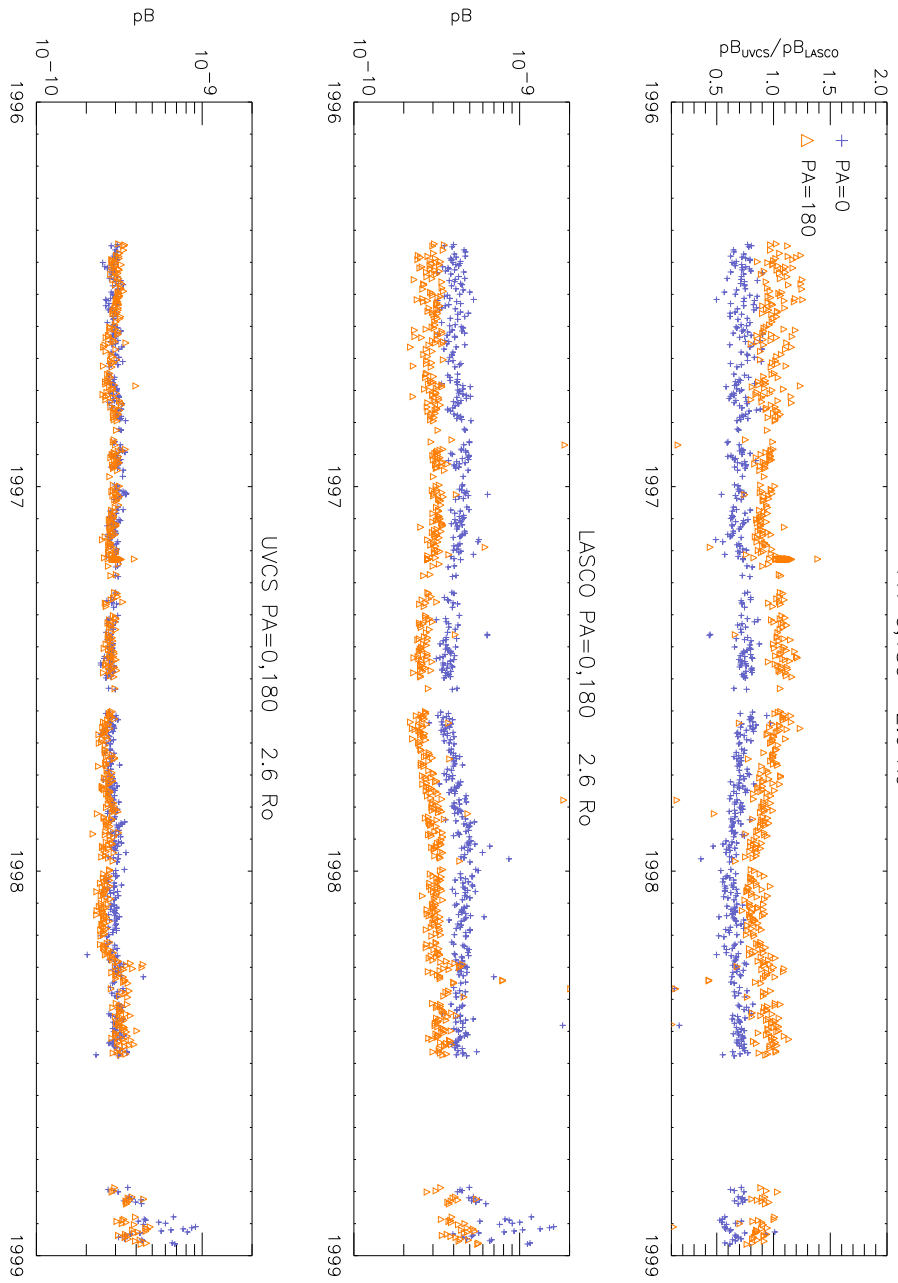

Figure 16.4: Time behavior plots of the coronal hole pBs, taken at position angles of 0 ° and 180° and at a height of 2.6 $R_{\odot}$. The top panel shows the pB ratio (UVCS/WLC to LASCO-C2), the middle panel shows the LASCO-C2 pBs, and the bottom panel shows the UVCS/WLC pBs. The orange triangles and blue crosses represent position angles of 0° and 180°, respectively. Note the systematic difference in between the north and south coronal hole pBs as seen by LASCO-C2.

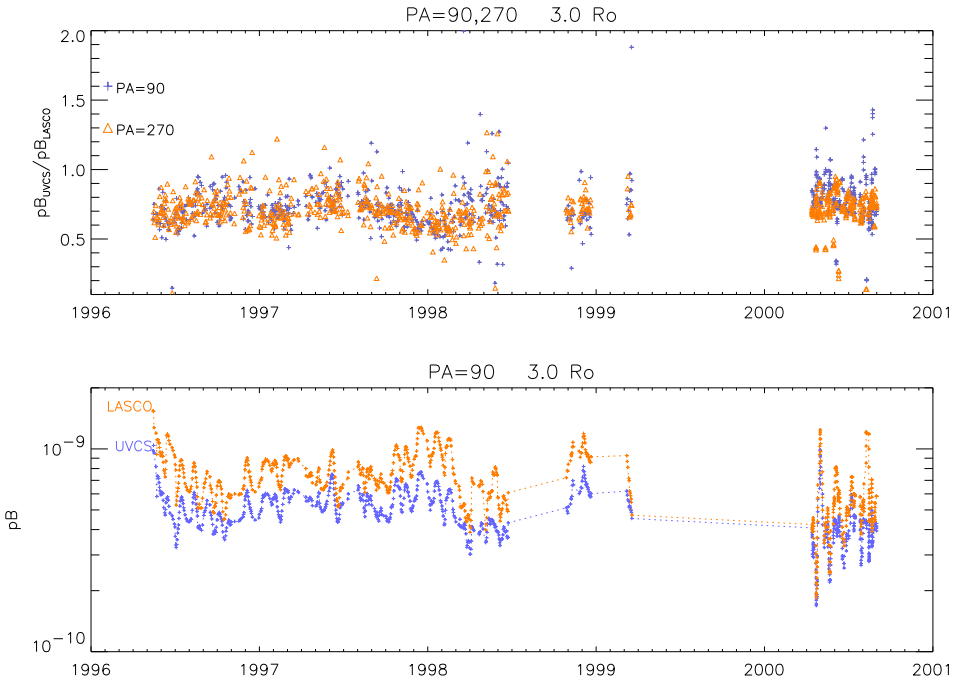

Figure 16.5: Time behavior plots of the equatorial pBs, taken at position angles of 90 ° and 270° and at a height of 3.0 $R_{\odot}$. The top panel shows the pB ratio (UVCS/WLC to LASCO-C2) and the bottom panel shows the individual UVCS/WLC and LASCO-C2 pBs.

Figures 16.4 and 16.5 illustrate the time behavior of LASCO-C2 and UVCS/WLC pB measurements. Figure 16.4 shows that the UVCS/WLC measurements in both the north and south coronal holes are more constant in time than the LASCO-C2 measurements. It is also interesting and puzzling to note that while the UVCS/WLC pB measurements in the north and south coronal holes are about equal, the LASCO-C2 measurements show a clear and systematic difference. Figure 16.5 is a similar plot, but made for the equatorial regions. There is not much evidence of any difference in the pB ratio above the east and west limbs.

16.4.3 UVCS/WLC and Spartan 201: Special Observations

Figure 16.6 shows the ratio of the UVCS/WLC pB to that of Spartan 201 during the STS-95 John Glenn Space Shuttle mission in November 1998. These data points show a ratio of about 0.8 at most heights. The data points with larger ratios (some of the asterisks), have poor simultaneity and weaker signals. The squares have much better simultaneity, larger signals and less UVCS/WLC stray light uncertainty. The median of the ratios denoted by the asterisks is 0.81, the mean is 0.83 and the standard deviation is 0.13. The median of the ratios denoted by the squares is 0.85, the mean is 0.76 and the standard

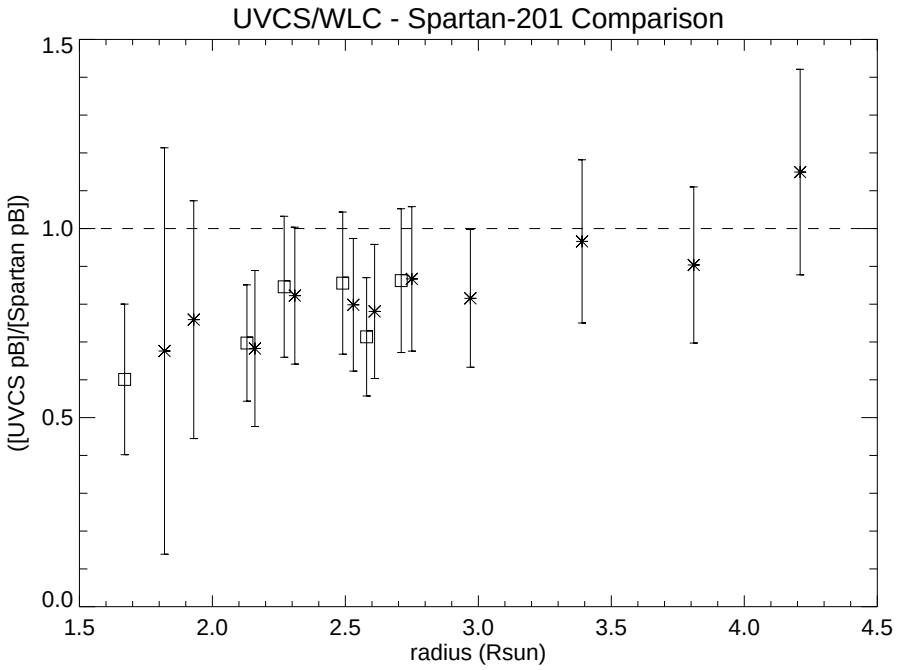

Figure 16.6: Ratio of the UVCS/WLC to the Spartan 201 White Light Coronagraph pBs for observations taken during the STS-95 John Glenn shuttle mission in November 1998. The data points represented by the squares have a stronger signal and better simultaneity than those represented by the asterisks.

deviation is 0.10.

16.5 Discussion

As was mentioned above, the median of all the ratios in Figure 16.1 is 0.79, the mean is 0.83 and the standard deviation is 0.25. The median relative standard uncertainty in the individual ratios is 33 % for heights below 2.9 $R_\odot$ and 15 % for heights above 2.9 $R_\odot$ (see Table 16.3). The difference of the mean pB values of the UVCS/WLC and LASCO-C2 when approximately co-registered is about 20 %. This difference can be explained by the described sources of uncertainty.

The asterisks in Figure 16.3 mark the median of the scatter distribution, and they show that the median value of the UVCS/WLC to LASCO-C2 pB ratio decreases with signal strength. The low ratios at high pB (typically found at low heights) could be explained by a systematic shift introduced by errors in the LASCO-C2 vignetting function at low heights where the correction is large. The high ratio at low pB (typically found at large heights) could be explained by incorrect stray light subtraction on the part of either or both instruments, or by the radiometric uncertainty being exceeded by the LASCO-C2

vignetting correction at low heights.

Figure 16.4 shows another curious trend: LASCO-C2 sees a difference in the coronal polarized radiance between the north and south coronal holes but UVCS/WLC does not. It is very difficult to explain this behavior in terms of the UVCS/WLC instrument, since it is a single pixel instrument that rotates about an axis to look at different position angles. This design makes the UVCS/WLC occulting geometry and stray light properties independent of position angle, as is described in Section 16.2.

Two possibilities that might explain the difference in polar pB values come to mind:

- LASCO-C2 has more polarized stray light in the north than in the south near 2.6 $R_\odot$, which was the only height at positions angles of 0° and 180° used for this comparison.
- The C2 vignetting function, which can be a function of position angle as well as radius [*Brueckner et al.*, 1995], is in fact different for position angles of 0° and 180° at 2.6 $R_\odot$, and different from the current calibration values.

Of the two possibilities considered, the second is not unlikely because the vignetting correction is quite large for 2.6 $R_\odot$.

Figure 16.6 shows that the UVCS/WLC pBs are generally in agreement with those of Spartan 201, within the uncertainties. The median of all of the ratios in the figure is 0.81.

Acknowledgements

The authors thank Mari Paz Miralles for helping with the UVCS pointing calculations. This work is supported by NASA under grant NAG5-10093 to the Smithsonian Astrophysical Observatory, by the Italian Space Agency, and by the PRODEX programme of ESA (Swiss contribution).

Bibliography

Brueckner, G.E., Howard, R. A., Koomen, M. J., Korendyke, C. M., Michels, D. J., Moses, J. D., Socker, D. G., Dere, K. P., Lamy, P. L., Llebaria, A., Bout, M. V., Schwenn, R., Simnett, G. M., Bedford, D. K., Eyles, C. J., The Large Angle Spectroscopic Coronagraph (LASCO), *Sol. Phys.*, **162**, 357, 1995.

Fineschi, S., O'Neal, R., and Modigliani, A., unpublished technical report, 1997.

Fisher, R.R., and Guhathakurta, M., SPARTAN 201 White Light Coronagraph Experiment, *Space Sci. Rev.*, **70**, 267, 1994.

Frazin, R.A., Ph.D. thesis. University of Illinois, Department of Astronomy, 2002.

Howard, R., personal communication, 2002.

Kohl, J.L., Esser, R., Gardner, L. D., Habbal, S., Daigneau, P. S., Dennis, E. F., Nystrom, G. U., Panasyuk, A., Raymond, J. C., Smith, P. L., Strachan, L., van Ballegooijen, A. A., Noci, G., Fineschi, S., Romoli, M., Ciaravella, A., Modigliani, A., Huber, M. C. E., Antonucci, E., Benna, C., Giordano, S., Tondello, G., Nicolosi, P., Naletto, G., Pernechele, C., Spadaro, D., Poletto, G., Livi, S., von der Lühe, O., Geiss, J., Timothy, J. G., Gloeckler, G., Allegra, A., Basile, G., Brusa, R., Wood, B., Siegmund, O. H. W., Fowler, W., Fisher, R., and Jhabvala, M., The Ultraviolet Coronagraph Spectrometer for the Solar and Heliospheric Observatory, *Sol. Phys.*, **162**, 313, 1995.

Kucera, T.A., personal communication, 2002.
Panasyuk, A.V., Three dimensional reconstruction of UV emissivities in the solar corona using the Ultraviolet Coronagraph Spectrometer data from Whole Sun Month, *J. Geophys. Rev.* **104**, 972, 1999.
Romoli, M., Frazin, R.A., Kohl, J.L., Gardner, L.D., Cranmer, S.R., Reardon, K., and Fineschi, S., In-flight calibration of the UVCS White Light Channel, this volume, 2002.
Solanki, S.K., Solar variability, this volume, 2002.
Wang, D., personal communication, 2001.